Lightweight Structures with Adaptive Dynamic Behavior Through Evanescent Morphing

Tom Ehrig, Christoph Hildebrand, Klaudiusz Holeczek, Niels Modler, and Pawel Kostka

1 Introduction

1.1 State of the Art

Improving the energy efficiency and achieving new performance levels of vehicles, machines and facilities is a continuous challenge for engineering and science. In the scope of structural design, a consistent implementation of lightweight design principles is widely recognized as an important tool to achieve this goal. Hybrid materials combining polymers, ceramics, lightweight alloys and composites as well as integral design with a reduced number of joints offer the possibility to develop light components with material type and distribution optimized for actual operating loads. An ultimately stiffness/strength-oriented design, however, often causes a problematic vibration susceptibility, especially of common thin-walled components and makes the application of additional damping measures necessary. Herein, some representative examples include:

T. Ehrig (✉) · C. Hildebrand · K. Holeczek · N. Modler · P. Kostka
Technische Universität Dresden, Institute of Lightweight Engineering and Polymer Technology, Holbeinstr. 3, 01307 Dresden, Germany
e-mail: tom.ehrig@tu-dresden.de

C. Hildebrand
e-mail: christoph.hildebrand@tu-dresden.de

K. Holeczek
e-mail: klaudiusz.holeczek@watttron.com

N. Modler
e-mail: niels.modler@tu-dresden.de

P. Kostka
e-mail: pawel.kostka@tu-dresden.de

P. Eberhard (ed.), *Calm, Smooth and Smart*, Lecture Notes in Applied and Computational Mechanics 102, https://doi.org/10.1007/978-3-031-36143-2_8

- special sandwich panel cores with layered damping materials [26] or filled with granular materials [17], including voids of optimized geometries [19],
- local dampers such as acoustic black holes [20], particle dampers [10, 21] and joints with viscoelastic damping [12],
- active magneto-/electro- or photorheological layers with the damping and stiffness controlled by magnetic, electric field or light, respectively [1, 9, 24],
- distributed active damping systems that use vibration sensors and actuators attached to complex-shaped structures, driven by real-time controllers [11, 18].

Common to active systems is a real-time calculation and generation of damping forces according to the instantaneous vibration position of the damped element. The necessary vibration measurement, signal routing, and a permanent power consumption combined with additional masses of the structure-integrated and external components often prove to be challenging and limit the application scope of active damping systems. Therefore, passive damping solutions are still used for a large part of technical applications. Especially free and constrained damping layers of viscoelastic materials are a widely used choice for flat panels, curved shell components [16] or structures with complex geometries [2]. A number of investigations aim at integration of such layers during the material manufacturing process [22] or at optimal distribution of damping segments [27].

In the case of widely used Constrained Layer Damping (CLD), a damping layer attached to the surface of a component is constrained by an additional top layer made of stiff material. Resulting shear deformations of the damping layer enable a particularly high damping power density of such treatment. However, the setup and material configuration of passive damping layers are typically designed for specific vibration conditions of the respective structures and do not allow any adaptation of their properties to varying excitation parameters.

1.2 Compressible Constrained Layer Damping

The presented research activities are pioneering work to develop a new kind of CLD, referred to as Compressible Constrained Layer Damping (CCLD) that implements a simple and almost massless mechanism for adaptation of damping properties. The conventional solid material of the viscoelastic layer is replaced here by a compressible one. The volume of the damping layer is considered as a structural cavity, which can be supplied with negative or positive pressure in order to control the damping layer thickness (Fig. 1) and thus the

- properties of the damping material - its densification or expansion affects the storage and loss shear modulus, G' and G'', respectively
- deformation kinematics of the layer - the shear deformation amplitude $\hat{\gamma}$ increases with the reduction of the thickness t_v.

Compared to typical active systems, the proposed actuating principle contains no explicit actuators. Instead, the damping layer itself or special structural cavities gen-

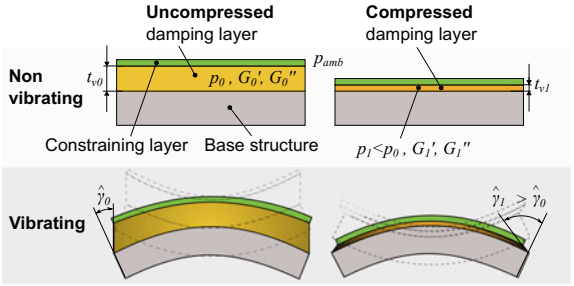

Fig. 1 The CCLD setup similar to the well-known CLD design, with the incompressible viscoelastic damping layer replaced by a compressible one. Actuating pressure $p_1 < p_0$ densifies the damping material and alters the shear deformation amplitude γ_1 due to variable damping layer thickness t_v

erate evanescent deformations when supplied with hydraulic fluid, compressed air or vacuum, which significantly reduces the implementation costs. In this way, the dynamic response of a CCLD-damped structure can be successively adapted on the basis of the current vibration conditions in order to achieve optimal dynamic response, e.g. in the sense of minimal vibration amplitude, minimal sound radiation, or maximal damping power etc. The term "evanescent deformation" used here refers primarily to the damping layer and it means such a geometrical change that it is irrelevant to the main function of the base structure. Additionally, curved base structures are subject to a certain degree of deformation and prestress caused by coupling effects due to CCLD actuation. These effects can also change the dynamic behavior and thus represent a part of the adaptation mechanism.

Considering the multiple phenomena and their interactions that occur in CCLD, the analysis of its adaptive damping properties as well as the elaboration of appropriate design guidelines require a complex work plan. The content of this chapter is structured accordingly as follows:

- Section 2 describes selection and characterization of compressible damping materials. Quasi-static and compression- and frequency-dependent viscoelastic properties of candidate materials are analyzed as a basis for understanding the damping layer behavior at various actuation conditions and vibration frequencies.
- Section 3 presents modeling and simulation approaches that use the acquired material data. First, an analytical model of simple beam structures is analyzed that allow a basic assessment of the CCLD potential as an adaptive damping treatment. Then, a parametric numerical model of a generic single-curved shell structure is described that explicitly includes both the complex deformation process during the CCLD actuation and the adaptive structural dynamic behavior.
- Further description focuses on experimental investigations on a lightweight single-curved shell structure with applied CCLD (Sect. 4). The experimental results are used at this stage for the validation of the developed numerical model.
- Finally, in Sect. 5 the application of the validated model for a simulation series is described. An assessment of the proposed damping solution is given based on a systematic variation of some CCLD key parameters.

2 Damping Materials

The following section describes the selection of suitable damping materials and their characterization. These steps were necessary for modeling purposes since neither compression-dependent material parameters for suitable materials were available in special literature nor were they provided by the manufacturers.

2.1 Material Selection

Even though a variety of viscoelastic materials are suitable for the application in a CCLD, the following material characteristics were identified as necessary for the realization of the CCLD principle:

- high damping to significantly influence the structural dynamic behavior,
- strong compression dependency of viscoelastic material properties for broad adjustment range of structural dynamic properties using evanescent morphing,
- high permeability for the actuation fluid and a technically feasible relation between compressive stress and compression, allowing an effective actuation,
- low density to suit the lightweight aspect.

The permeability for the actuation fluid significantly limits the material choice, making flexible open-cell foams a feasible material group. A product survey of commercial foams revealed the unavailability of sufficient quantitative specifications of material properties related to the above mentioned characteristics, hampering a direct selection of suitable materials. Especially the pressure-compression-shear damping/stiffness characteristics as a parameter of key importance could not be found for any compressible material even in specialized scholar publications. Therefore, a preselection of materials was conducted taking into account merely the available information about basic material features and the final selection was made based on the self conducted experimental material characterization.

Since the material density is an important lightweight indicator and it influences the damping as well as determines indirectly the actuation-relevant porosity of the foam, a broad range of densities was used as an initial material selection criterion. This led to the selection of twelve open cell polyurethane (PU) foams and a single melamine foam,[1] samples of which were procured and subjected to an in-house quality control and preliminary rheometric tests. Finally, three PU foams and the melamine foam with favorable viscoelastic properties and significantly different property profiles were used in further investigations.

Another material group that fulfills the criteria mentioned above are nonwovens. Since the production of nonwovens converts the fibers directly into fabrics and thus eliminates the yarn production process, nonwovens are a very cost-effective solution for many applications. Low density and remarkable energy absorption capacity are

[1] As a material with fundamentally different open cell morphology compared to PU foams.

Table 1 For the in-depth investigation selected foams and nonwovens

Sample	Type name	Manufacturer	Base material	Density kg/m^3
Foam A	Basotect® G+	BASF SE	Melamine resin	9.0
Foam B	RG1720	Schaumstoffe W. Wegerich GmbH	PU	16.3
Foam C	Visco 5030	Schaumstoffe W. Wegerich GmbH	PU	48.4
Foam D	Confor™ M CF40	Aearo Technologies LLC	PU	96.2
Nonwoven A	PP05	MK Filze GmbH	100 % PP fibers	120
Nonwoven B	PES 03-36	Filzfabrik Gustav Neumann GmbH	100 % PET fibers	360
Nonwoven C	Woll05	MK Filze GmbH	90 % wool fibers 10 % staple rayon	280
Nonwoven D	Nomex®	Filzfabrik Gustav Neumann GmbH	100 % meta-aramid fibers	160

the reasons why nonwovens have been used for years for acoustic or impact damping [15]. Although it seems likely that the superior energy absorption capacity could also be used for structural dynamic damping, there are only a few publications on the use of nonwovens or dry fiber assemblies for vibration damping. Nonwovens made of four main representative materials have been chosen (cf. Table 1):

- Polypropylene (PP) fibers as low density material, used e.g. for sound/heat insulation and soundproofing of loud-speakers or in vehicles,
- Polyethylene terephthalate (PET) fibers, as a low-cost, often recycled material,
- Wool fibers, as a renewable raw material, and
- Aramid fibers, which are known for their good damping properties e.g. in fiber composite materials and have a high temperature and chemical resistance.

2.2 Material Characterization

The CCLD-relevant properties were determined for the materials given in Table 1 based on procedures described in DIN EN ISO 845:2009-10 (density), DIN EN ISO 11357-2:2014-07 (glass transition temperature), and ASTM D 3576 (cell diameter of PU foams; due to different morphology, a similar procedure was derived for the melamine foam). In addition, microscope images were analyzed for all materials to evaluate the microstructure. For the nonwovens, also fiber diameter and fiber distribution were determined from these images.

The experiments related to the compression behavior and viscoelastic shear properties were conducted using an universal testing machine (Z2.5, Co. Zwick-Roell) respectively a rotatory rheometer (MCR 502-300, Co. Anton Paar) in parallel plate mode. Detailed information regarding the characterization of the foams can be found in [7], of the nonwovens in [8].

2.2.1 Quasi-static Material Properties

The quasi-static through thickness compression behavior, which determines the actuation characteristics of the CCLD, was investigated by uniaxial compression tests. Throughout this chapter, the compression level k is defined as:

$$k = \left(1 - \frac{t_{v1}}{t_{v0}}\right) \cdot 100\% \tag{1}$$

where t_{v1} and t_{v0} are the sample thicknesses in the compressed and uncompressed state, respectively. For an initial comparison of the materials, the nominal compressive stress as a function of the compression level is shown in Fig. 2. For the sake of clarity and due to the good repeat accuracy, only one loading cycle is presented. All investigated materials show a quantitatively similar, non-linear behavior, however, they can be compressed to different levels. For an adaptive damping system, this means that nonwovens reveal a smaller range of the compression level due to a pressure-driven actuation. This, in turn, leads to lower deformations of the structure, which is well compatible with the idea of evanescent morphing. The results shown later in this section, however, confirm that even such small deformations lead to significant changes in viscoelastic properties. For the tested foam materials, three typical regions [25] can be distinguished: cell wall bending, cell wall buckling and foam densification (shown exemplary for foam D in Fig. 3). It could be observed that all of the tested foams could be densified at least up to 88 % using atmospheric pressure.[2] In order to understand the deformation kinematics and to assess the compression reversibility at such high densifications, high-resolution in situ computed tomography (CT) enabling x-ray scanning in deformation controlled mode, was used (Fig. 3). It was found that even if the tested foams were compressed to one tenth of their initial thickness, they would return to their undamaged initial structure after relief.

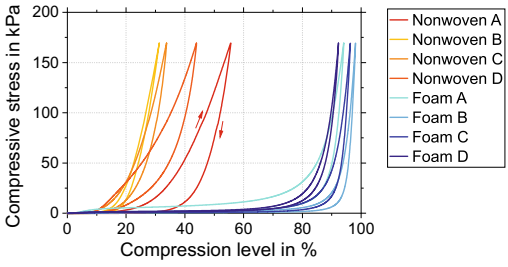

Fig. 2 Nominal compressive stress versus compression level k for loading and unloading at uniaxial compression. The flexible foams could be compressed to significantly higher levels at comparable compressive stress as nonwovens

[2] Which is a theoretical limit in the case of a vacuum actuation.

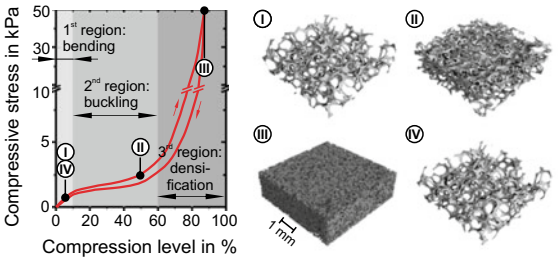

Fig. 3 Nominal compressive stress versus compression level k with in situ CT images of foam D at (I) 5 %, (II) 50 %, (III) 88 % compression and (IV) after relief of the compression force again at 5 % compression

2.2.2 Compression- and Frequency-Dependent Material Properties

In the scope of material characterization and following modeling of the structural dynamic behavior, a linear viscoelastic model of the foams as damping material was assumed at individual compression levels. This assumption was verified based on the analyses of raw rheometric data revealing harmonic, phase shifted stress response on applied harmonic strain. Therefore, the well established description of the viscoelastic properties using the complex shear modulus $G^* = G' + iG''$ was applied, where G' is the stiffness related storage modulus and G'' is the damping related loss modulus. The compression-dependent complex shear modulus—determining the adaptability of the CCLD treatment—was characterized in shear rheometric tests at different frequencies and temperatures for several compression levels with compressive stresses up to 100 kPa, anticipating a vacuum driven CCLD actuation.

In the case of foam materials, the time-temperature superposition (TTS) principle allowed a transformation of the test data in an augmented frequency range that is much broader than the testing machine's frequency span (here 0.1 ... 16 Hz). The spans of test temperatures and frequencies were selected in such a way that the measured data could be extrapolated for a fixed operating temperature of 23 °C into a new frequency range ending at 10^4 Hz, what required several thousand independent rheometric tests. Figuer 4 is provided to illustrate the frequency- and compression-dependent behavior of the storage shear modulus and the loss factor for foam D. The characterization of foams A-D is described in detail in [7].

Figure 5a shows an example of the characteristic hysteresis behavior for a foam and a nonwoven as determined with the rheometric investigations. The enclosed area of the loops is proportional to the energy dissipated per cycle. As can be seen, nonwovens have a significantly higher energy dissipation capacity than foams. The influence of the compression level is shown exemplary in Fig. 5b for nonwoven A. With increasing compression, all materials show an increase of the stiffness on the one hand and an increase of the dissipated energy on the other hand. Nonwovens, however, revealed an even stronger dependence of shear damping and stiffness upon compression. Further advantages of nonwovens are almost frequency-independent material behavior

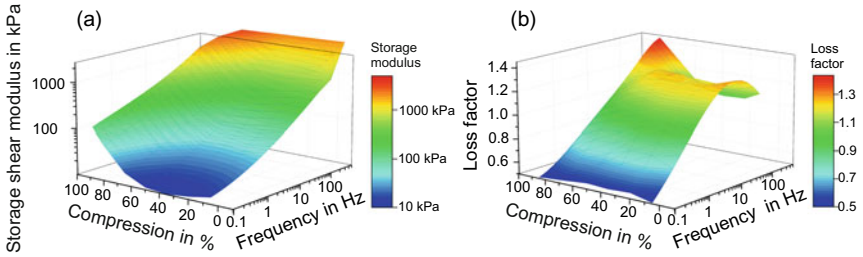

Fig. 4 **a** Storage shear modulus and **b** loss factor versus compression and frequency of foam D [4]

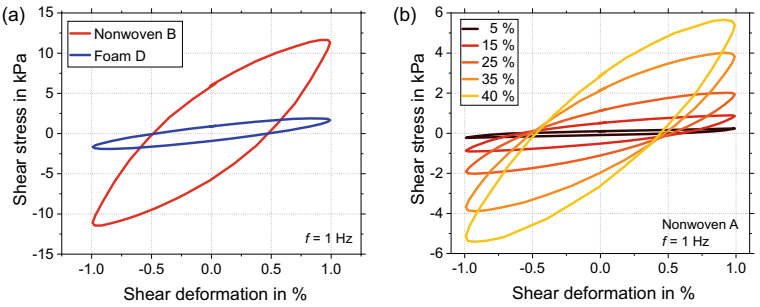

Fig. 5 **a** Comparison of the shear stress versus shear deformation for foam D and nonwoven B at comparable compressive stress; **b** variation of the compression level k from 5 to 40 % for nonwoven A, which showed the strongest dependency of shear damping and stiffness upon compression

at room temperature (except for nonwoven A made of PP) and significantly less temperature-dependent behavior.[3] However, nonwovens reveal a non-linear material behavior already at significantly smaller shear deformation amplitudes. This is due to the fundamentally different damping mechanism, which is mainly based on friction between the entangled fibers, and presents a challenge for modeling and design of a potential damping element. A more detailed discussion of the above mentioned effects can be found in [8].

Regarding the shear oscillation motion, an insignificant volume change during a vibration period was assumed, which should result in a low impact of fluid flow effects on damping properties. Thus, the influence of effects connected with fluid flow in the cell skeleton was neglected in the above presented material characterization.

2.2.3 Characterization at High Excitation Parameters

In addition to the above-described tests at low excitation parameters, effects occurring at high excitation amplitudes and frequencies were investigated. For these investiga-

[3] In fact, this is also the reason why TTS is not feasible with most nonwovens.

tions a test stand was developed and used in connection with a large electrodynamic shaker (V8-440, Co. Bruel&Kjœr) generating a broad range of vibration amplitudes and frequencies (up to 1000 Hz). After a virtual dimensioning and fundamental experimental tests, an add-on module for simple-shear tests, based on the inertial mass principle, was extensively tested and put into operation. With this test stand it is also possible to characterize the damping materials to the point of damage in order to determine the limits of the CCLD. A primary result of the conducted material characterization is a catalog of material data describing compression- and frequency-dependent properties of several foams and nonwovens. These results, revealing a complex picture, can be used as the necessary basis for the modeling and simulation of structures with CCLD in an extended range of excitation parameters.

3 Modeling of Lightweight Structures with CCLD Treatment

For a detailed analysis of the CCLD influence on the dynamic behavior of lightweight structures, models with different abstraction levels have been realized. First, an analytical model of bending beams and its application in exemplary parameter studies are described (Sect. 3.1). Then, further models were developed, e.g. with prestressed beams [13], which cannot be discussed here in detail due to limited space. Finally, the latest and most complex model–a fully parametric finite element (FE) model for single-curved shell structures–is presented in Sect. 3.2.

3.1 Analytical Model for a Simply Supported Beam with CCLD

For the analytical approach, a well established mathematical formulation of a simply supported beam with CLD [28] has been modified by adding the possibility of a compression-driven adaptation of the geometrical and material properties of the viscoelastic layer. This was accomplished by implementing the compression dependent properties of the viscoelastic layer: its thickness, mass density as well as storage and loss shear modulus.

The model was used in a series of simulations to study the CCLD potential regarding the damping capacity and its adaptation as well as to understand the physical relationships of parameters describing the system configuration. The length ($L = 550$ mm) and the width ($W = 55$ mm) of the base beam made of carbon fiber reinforced epoxy resin was kept constant while its thickness h_b was varied in such a way that its slenderness took the values of 10, 20 and 100. The thickness of the constraining layer, made of the same material as the base beam, was kept constant at 0.25 mm. The parameters of the viscoelastic layer were consecutively set according to material

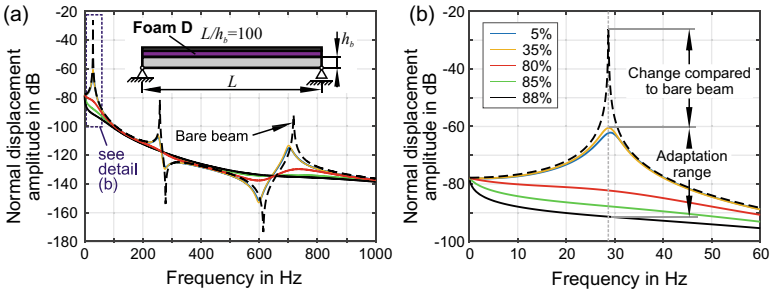

Fig. 6 Exemplary normal amplitudes at the beam's middle point $L/2$ calculated using the analytical model from [14]: **a** Comparison of the vibration amplitudes of the bare beam (dashed line) and beam with CCLD at different compression levels, **b** detailed view of the frequency range around the 1st eigenfrequency and graphical explanation of the key CCLD efficiency indicators

characterization results for the foams shown in Table 1. Since the shear deformation of the viscoelastic layer during the beam bending vibrations increases with the decrease of its thickness (cf. shear deformation amplitude γ_1 in Fig. 1), possibly thin layers were pursued in order to maximize the damping effect. Thus, the lower thickness limit in uncompressed state was set for each foam to exactly 10 mean foam cell diameters.

The normal displacement amplitude at the beam's middle point $L/2$ as a response to a unit, normal harmonic excitation force applied in the same point was calculated for every above mentioned slenderness value and foam material. The change of the dynamic behavior in comparison with the bare beam behavior and the adaptation range as a result of the CCLD actuation, were used as key effectiveness indicators. They are presented for an exemplary system configuration in Fig. 6. Results for other configurations are compactly presented in Fig. 7 for the bending modes 1, 3 and 5. A detailed description of the model used and a thorough discussion of the results can be found in [14]. The results of the simulations described up to this point confirm the principal correctness of the initial theoretical assumptions about the adaptive dynamic behavior of structures with CCLD treatment. Both significant vibration damping and the CCLD adaptability through effects occurring during compressive actuation of the damping layer were observed. The developed analytical modeling approach can be used for a quick preliminary system design. However, due to the complexity of real-world structures, more elaborate modeling is often required.

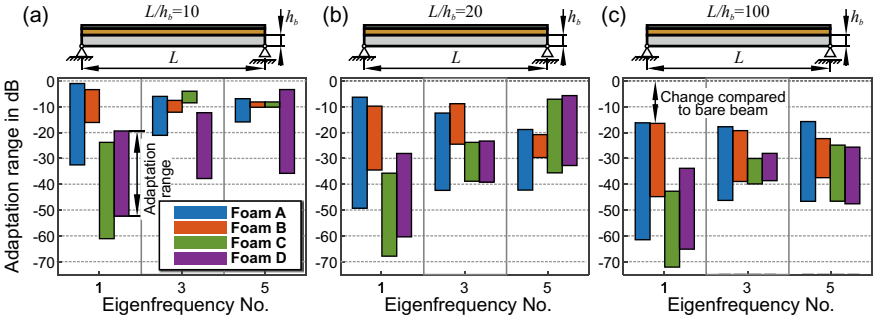

Fig. 7 Adaptation ranges of the CCLD-beam's dynamic behavior in comparison with the bare beam behavior for different foam materials and slenderness values: **a** 10, **b** 20 and **c** 100 [6]

3.2 Numerical Model for Single-Curved Structures with CCLD

A multi-step FE model was developed to estimate the potential of CCLD for single-curved structures. In the following, the setup of the model is described and a possible indicator to estimate the efficiency of the CCLD, the mean mobility, is discussed.

3.2.1 Setup of the Parameteric FE Model

The key component of the model is a two-step simulation procedure which was implemented in the commercial software COMSOL Multiphysics® 5.6 (Fig. 8). This simulation procedure is re-run with adapted input data for each set of selected CCLD design parameters. The modeled geometry was discretized using quadrilateral elements for the damping and constraining layer as well as tetrahedral elements for the base structure to reduce computation time. The different layers are modeled as union, therefore no relative motions of the layers to each other are possible. The model boundary conditions are defined as a pressure load on the damping layer and a fixed- and floating constraint on two opposing axial edges of the base structure.

In the first step, the deformation and the prestress, caused by the compression of the damping layer material by the CCLD-actuation, are computed using a stationary solver (no damping is taken into account). For a realistic simulation of the large material deformations, the hyperelastic Storaker model [23] was selected for the damping layer. For the fitting of the Storaker model, data sets from uniaxial compression tests mentioned in Sect. 2.2.1 were used separately for each considered foam material (cf. Table 1). A sample validation of the model was performed on a real CCLD setup assembled with foam D. The deformation behavior of the CCLD actuated in the pressure-controlled mode was measured with a 3D scanner and compared with the model outputs of this simulation step. Due to the good agreement, the described modeling approach was used in all further described simulations.

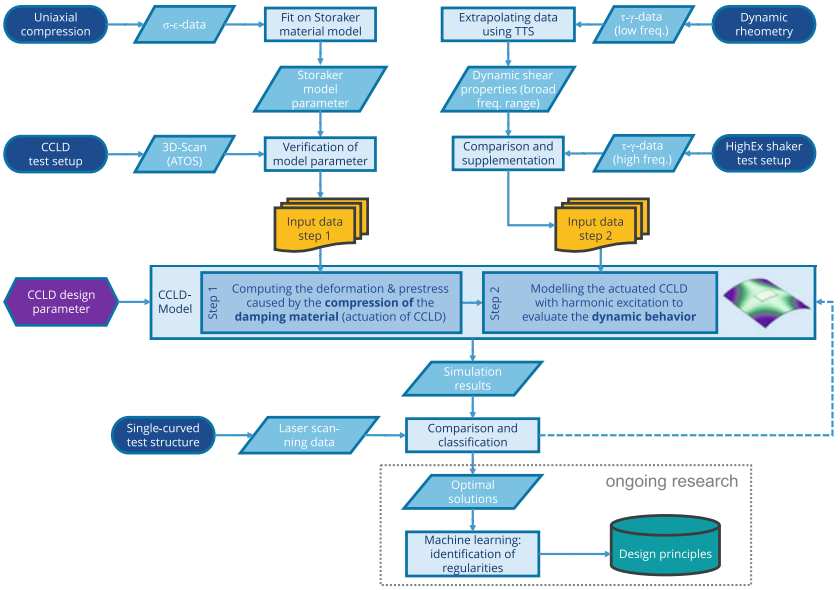

Fig. 8 Overview of the parametric FE model with input-output data

In the second step, the deformed and prestressed CCLD from the first step is taken over for a harmonic response analysis. Stationary vibration responses to a monoharmonic force excitation are simulated in a selected frequency range. To reduce simulation time, an adaptive control of the frequency step was implemented. In this simulation step, the damping layer material is switched to linear elastic material and parametrized with frequency-dependent values of shear modulus and loss factor (Sect. 2.2.2) taking into account the previously calculated compression level.

For the validation of the simulation results from this two-step simulation procedure, a single-curved test structure was manufactured and the simulation results were compared to the experimental data (Sect. 4).

3.2.2 Mobility as Indicator of CCLD Treatment Efficiency

To evaluate the impact of the proposed CCLD on the dynamic behavior of a structure, a variety of possible indicators can be defined. In this study, the mobility as a complex-valued frequency response function describing velocity per unit force was assessed. Therefore, the measured excitation force $F_{exc}(\omega)$ and response velocities $v(\omega)$ were used to calculate the mobility $M(\omega)$ as following:

$$M(\omega) = \frac{v(\omega)}{F_{exc}(\omega)} \tag{2}$$

The magnitudes of the mobilities at measurement points n were then averaged:

$$\bar{M}(\omega) = \sqrt{\frac{1}{N}\Sigma_{n=1}^{N} M_n(\omega)^2} \tag{3}$$

Here, $\bar{M}(\omega)$ is the mean mobility magnitude as a single convenient measure, which allows an assessment of the damping efficiency. N is the number of the velocity measurement points. It should be noted that the mobility is actually defined as the velocity that is perpendicular to the surface in relation to the excitation force. For the investigated curved structure, only the z components of the velocities[4] were taken into account to improve the comparability of the velocities measured by the laser scanning vibrometer and the simulation results.

4 Experimental Setup for Model Validation

The proof-of-principle for the CCLD treatment was performed in an earlier investigation phase on a flat panel structure and revealed very promising results [5]. In this section, the experiments on a single-curved shell structure are presented and the results are compared with the developed model.

4.1 Configuration of the Curved CCLD Sample Structure

The analyzed base structure is a cylindrical shell section with a constant radius r_b, thickness t_b, width w_b and section angle ϕ_b precisely milled from aluminum (EN AW-5083). This expensive manufacturing solution guarantees very high geometric precision and residual stress-free condition of the base structure, avoiding a number of random effects that could influence the observed vibration behavior. The CCLD treatment was set up as shown in Fig. 9. The CCLD patch was applied only partially and has a width w_v and section angle ϕ_v. The viscoelastic damping layer consists of the open-cell PU foam D with the thickness t_v depending on the compression level. An aluminum sheet with the thickness t_c was used as constraining layer. The additional mass due to the CCLD patch was only 0.12 kg (+4.36 %). The vacuum-sealing was assured by using a vacuum film, which was glued to the base structure and the constraining layer. To avoid introducing another viscoelastic layer and to exclude further phenomena such as curing of the adhesive in the open-cell pores, the individual layers were not glued together. The structure was held in position by the tightly applied vacuum film and later fixed by the actuation pressure, which enabled

[4] This refers to the components of the vibration velocities that are perpendicular to a plane defined by the corner points of the curved shell.

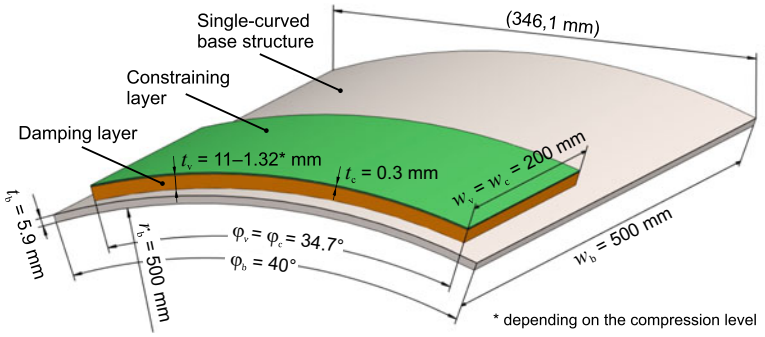

Fig. 9 Schematic drawing of the CCLD setup on a single-curved structure

Table 2 Applied actuation pressure and corresponding damping layer thickness ($t_{v0} = 11$ mm)

Applied actuation pressure p_{act}	–1.1 kPa	–2.4 kPa	–5.4 kPa	–16.9 kPa	–31.7 kPa	–49.0 kPa
Damping layer thickness t_v	$0.95\,t_{v0}$	$0.65\,t_{v0}$	$0.35\,t_{v0}$	$0.2\,t_{v0}$	$0.15\,t_{v0}$	$0.12\,t_{v0}$
Compression level k	5 %	35 %	65 %	80 %	85 %	88 %

the coupling of the layers by frictional forces.[5] The applied actuation pressure was generated by a vacuum pump and adjusted with a valve to achieve the predetermined compression levels (Table 2).

4.2 Measurement Setup

The characterization of the dynamic behavior was carried out on the test structure hung up on an auxiliary frame, mounted on a vibration-insulated table (Fig. 10). An electrodynamic shaker (type 4810, Co. Bruel&Kjœr) was used to generate a sine sweep excitation force in the frequency range between 50 and 450 Hz. This force, applied near a corner of the base structure, was measured with an impedance head (type 8001, Co. Bruel&Kjœr). At the same time, the vibration response was recorded by means of a laser scanning vibrometer (type PSV-400, Co. Polytec) at 35 regularly distributed laser light reflecting spots, with a resolution of 48.9 mHz.

Several test series were carried out, first with the base structure without CCLD and then with the applied CCLD patch. The compression levels were set in increasing, decreasing and random order, according to values shown in Table 2. The repeat

[5] The simulation results (Sect. 4.4) show a remarkably good agreement especially for the lowest compression level ($k = 5\,\%$), which supports this assumption.

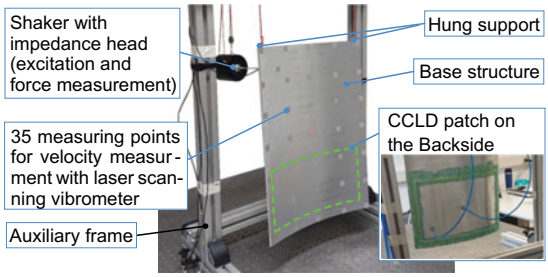

Fig. 10 Illustration of the measuring setup with the adaptive structure [4]

accuracy of all these measurements was excellent, so that only one measurement per compression level is used in the following discussion.

4.3 Discussion of the Measurement Results

4.3.1 Measured Mean Mobility at Different Compression Levels

The two simultaneous and compression-dependent phenomena: variability of material properties of the damping layer and its changing deformation kinematics (cf. Sect. 1.2) suggest a complex effect of the CCLD actuation on the dynamic behavior of the adaptive structure. Figure 11a shows the mean out-of-plane mobility (cf. Eq. 3) of the adaptive CCLD structure at different compression levels for the measured frequency range from 50 to 450 Hz, compared with the mean mobility of the bare base structure. Figure 11b and c provide a detailed illustration of the frequency range around the 2nd and 5th eigenfrequency (EF), respectively. Due to the additional mass of the CCLD patch, the EFs shift to a lower frequency range at low compression levels of the damping layer. Increasing shear stiffness at higher compression levels compensates this effect, and the EFs shift back to a higher range.[6] A significant reduction of the amplitudes compared to the base structure can be observed, but the relationship between compression level and reduction of the amplitude is rather complex. In the example shown, the amplitude of the 5th EFs decreases steadily with increasing compression (Fig. 11c), while the amplitude of the 2nd EF reaches its minimum amplitude at a compression level of 80 % (Fig. 11b).

4.3.2 Compression Level for Achieving the Minimal Mobility

The effect of CCLD in an adaptive mode of vibration damping can be illustrated by the example of the presented structure under a monoharmonic vibration excita-

[6] The reduction of the bending stiffness of the adaptive CCLD structure, caused by a decrease of the second moment of inertia with increasing compression, appears to play a minor role.

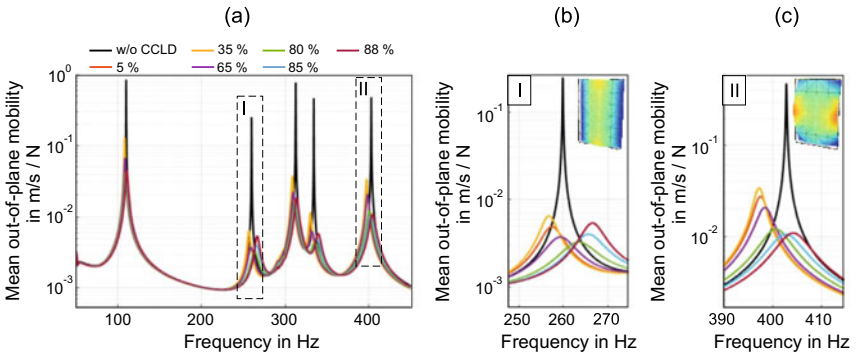

Fig. 11 **a** Mean out-of-plane mobility for different compression levels; **b**, **c** detailed view of the 2nd EF and the 5th EF (legend is valid for all three figures) [4]

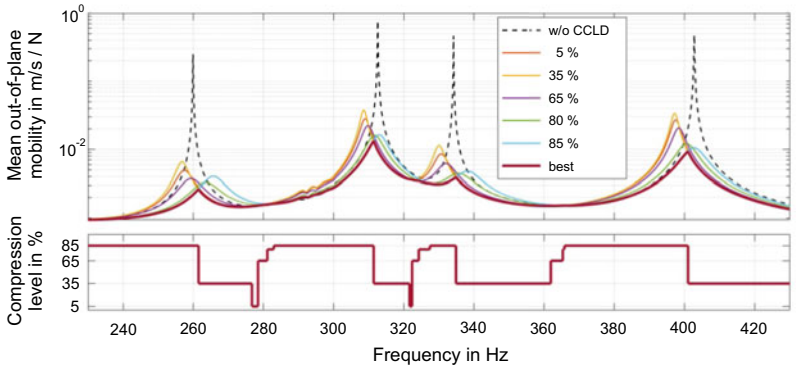

Fig. 12 Mean out-of-plane mobility for different compression levels and controlled state with the minimal achievable mobility (bold line) by adapting the compression level (step diagram)

tion. Figure 12 extends the mean mobility patterns by a step diagram showing the frequency-dependent compression level of the CCLD yielding the minimum mobility. This actuation profile, which includes all the levels analyzed, allows a significant calming of the sample structure (bold line) compared to the respective constant compression levels. In addition to minimum mobility, other criteria for CCLD control are also possible, e.g. maximum damping power, minimum sound radiation, etc. The CCLD control in technically common, more complex excitation scenarios remains a challenging task that will not be addressed here.

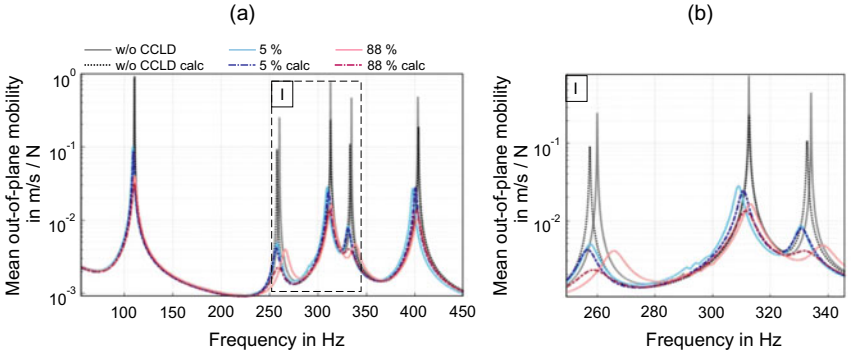

Fig. 13 Measured mean out-of-plane mobility (solid lines) compared to the simulation results (dotted lines) for **a** the measured frequency range and **b** detail of the 2nd to 4th EF [4]

4.4 Comparison of Experimental and Simulation Results

Achieving a good quantitative agreement between experimentally determined and simulated vibration properties in terms of natural frequencies and vibration amplitudes is often challenging in the case of more complex structures. In the present case, an additional difficulty results from the modeling of the CCLD actuation process that modifies many properties at material, geometric, and kinematic level.

In a first step of the validation procedure, the model and experiment outputs in terms of the mean mobility were compared for the bare structure. The actual validation step concerned a similar comparison at different CCLD actuation states. An example of experimental and simulated patterns for the two steps is shown in Fig. 13. The obtained results were evaluated as satisfactory and the model as valid for further simulation-based analysis of CCLD effect in other system configurations. A more detailed discussion on the validation procedure can be found in [4].

5 Model Application

The results shown in Sect. 4 demonstrate that CCLD can be an effective damping treatment. However, determining the optimal CCLD layout for a given use case appears to be a challenging task due to a large number of design parameters, including:

- Dynamic behavior the base structure,
- Number, distribution and geometry of CCLD patches (c.f. Fig. 9 as example),
- Material parameters, including (i) frequency-dependent, (ii) compression-dependent and (iii) temperature-dependent material behavior of the damping layer,
- Vibration excitation parameters.

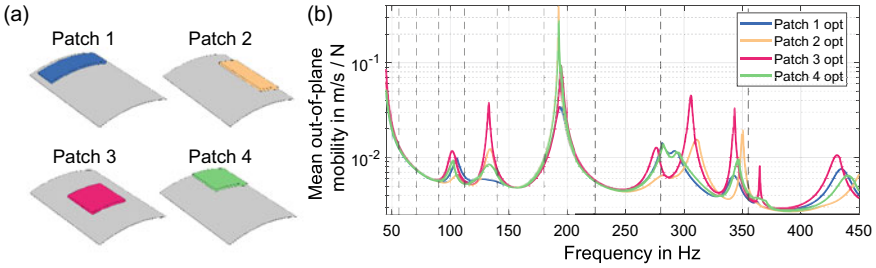

Fig. 14 **a** Schematic illustration of the four variants and **b** their mean out-of-plane mobility with adaptive control to achieve the minimal mobility

Furthermore, an optimal design depends on the respective objective function such as minimum vibration amplitude, minimum sound radiation, or maximum damping power, as well as on possible constraints including allowed space, position, and mass of the damping components. In the scientific approach followed here, a numerical experiment will be performed to comprehensively characterize the dynamic behavior under different parameter combinations. The results obtained will serve as the basis for a data-driven identification of CCLD design principles.

To illustrate the complex nature of the described task, an exemplary study will be presented. For a given base structure, only the position, width and section angle of the CCLD patch are varied. In all four variants shown in Fig. 14a, the CCLD patch has the same area and the additional mass in relation to the base structure is only 5 %. All other parameters remain constant in this study. Figure 14b illustrates the best possible condition i.e. the lowest mean out-of-plane mobility as described in Sect. 4.3.2. The responses for a monoharmonic excitation are obtained by successive control of the compression level for each of the four variants. It is clearly visible that the different patch configurations significantly influence the mobility, especially in the range of the EF's. Thus, with Patch 2, the EF at approx. 100 Hz can be damped effectively, whereas the EF at approx. 130 Hz can be damped significantly less. For Patch 1, on the other hand, the situation is exactly the opposite. The range between approx. 260 Hz and 380 Hz illustrates a similar effect particularly well. The vertical lines in Fig. 14b mark the 1/3 octave bands. A possible quantitative measure for the CCLD assessment can be the integrated mean out-of-plane mobility e.g. over 1/3 octave bands (Fig. 15). It is apparent that for the given CCLD parameters, the variant with Patch 1 is the best choice in the considered frequency range. However, it also becomes clear that, depending on the frequency range of interest, different variants are the best option. This small insight with only a few parameter sets already reveals a complex picture and should demonstrate the necessity of a large-scale parameter study.

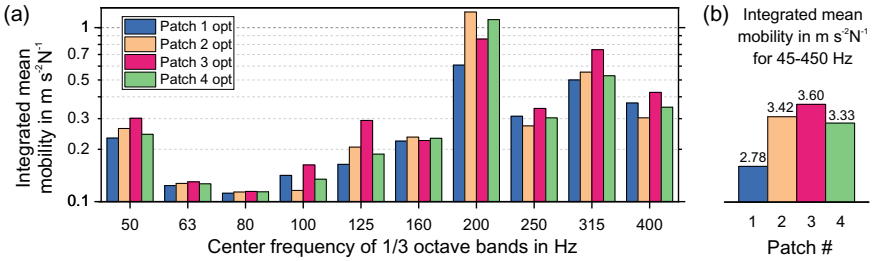

Fig. 15 **a** Comparison of the mean out-of-plane mobility integrated over the 1/3 octave bands for the four patch variants and **b** comparison of the mean out-of-plane mobility integrated over the entire frequency range (45–450 Hz)

6 Conclusion

The novel CCLD damping technique poses an efficient and nearly weight neutral solution to calm vibrating lightweight structures. In experiments carried out on a single-curved shell structure with a partial CCLD coverage and adaptive CCLD control it was possible to significantly reduce the maximum vibration amplitudes with only a small increase in the structure's mass. In order to choose suitable damping materials for the CCLD technique, different viscoelastic foams and nonwovens were investigated, characterized and necessary material properties were identified. In addition to the experimental investigations, a two-step simulation procedure was proposed and investigated. The therefore developed model uses the experimentally obtained material properties and is capable of predicting the structural dynamic behavior of a structure with applied and actuated CCLD. It shows a good agreement with the experimental results. This model provides the basis for a large-scale parameter study in the future. The hereby obtained results will then be used to develop guidelines for the design of CCLD patches and identify optimal CCLD design parameters like patch size, -position and -material. Further experiments with the test structures in different scenarios, such as in acoustic damping context [3] are planned.

References

1. Cho, M., Kim, J., Choi, S., Kim, G.: Non-contact tunable damping of a cantilever beam structure embedded with photo-rheological fluids. Smart Mater. Struct. **25**(2) (2016)
2. Dannemann, M., Täger, O., Modler, N.: Combined semi-analytical and numerical vibro-acoustic design approach for anisotropic fibre-reinforced composite structures. J. Sound Vib. **404**, 1–14 (2017)
3. Ehrig, T., Dannemann, M., Luft, R., Adams, C., Modler, N., Kostka, P.: Sound transmission loss of a sandwich plate with adjustable core layer thickness. Materials (Basel, Switzerland) **13**(18), 4160 (2020)
4. Ehrig, T., Hildebrand, C., Modler, N., Kostka, P.: Modelling and experimental verification of a curved lightweight structure with adaptive dynamic behaviour. In: Proceedings of the 28th International Congress of Sound and Vibration, ICSV 2022 (2022)

5. Ehrig, T., Holeczek, K., Kostka, P.: Experimental investigations of lightweight structures with fluidically actuated Compressible Constrained Layer Damping. Mater. Today Commun. **16**, 204–211 (2018)
6. Ehrig, T., Holeczek, K., Modler, N., Kostka, P.: Dynamic behaviour adaptation of lightweight structures by compressible constrained layer damping with embedded polymeric foams and nonwovens. Appl. Sci. **9**(17) (2019)
7. Ehrig, T., Modler, N., Kostka, P.: Compression and frequency dependence of the viscoelastic shear properties of flexible open-cell foams. Polym. Test. **70**, 151–161 (2018)
8. Ehrig, T., Müller-Pabel, M., Modler, N., Kostka, P.: Experimental investigations on compressed nonwovens as damping material for enhanced constrained layer damping. In: Proceedings of the 28th International Congress of Sound and Vibration, ICSV 2022 (2022)
9. Eshaghi, M., Sedaghati, R., Rakheja, S.: Dynamic characteristics and control of magnetorheological/electrorheological sandwich structures: a state-of-the-art review. J. Intell. Mater. Syst. Struct. **27**(15), 2003–2037 (2016)
10. Gnanasambandham, C., Fleissner, F., Eberhard, P.: Enhancing the dissipative properties of particle dampers using rigid obstacle-grids. J. Sound Vib. **484** (2020)
11. Haase, T., Unruh, O., Algermissen, S., Pohl, M.: Active control of counter-rotating open rotor interior noise in a Dornier 728 experimental aircraft. J. Sound Vib. **376**, 18–32 (2016)
12. Hammami, C., Balmes, E., Guskov, M.: Numerical design and test on an assembled structure of a bolted joint with viscoelastic damping. Mech. Syst. Signal Process. **70–71**, 714–724 (2016)
13. Holeczek, K., Koschichow, R., Schlieter, T., Ehrig, T., Kostka, P.: Numerical investigations of polymer-based fibre-reinforced structures with fluidically actuated Compressible Constrained Layer Damping. PAMM **18**(1) (2018)
14. Holeczek, K., Zhou, B., Kostka, P.: Evanescent morphing for tuning the dynamic behavior of composite lightweight structures: theoretical assessment. Mech. Adv. Mater. Struct. **10**(2), 1–107 (2019)
15. Karthik, T., Prabha-Karan, C., Rathinamoorthy, R.: Nonwovens: Process, structure, properties and applications. Woodhead Publishing India in textiles, WPI Publishing (2016)
16. Kliem, M., Høgsberg, J., Vanwalleghem, J., Filippatos, A., Hoschützky, S., Fotsing, E., Berggreen, C.: Damping analysis of cylindrical composite structures with enhanced viscoelastic properties. Appl. Compos. Mater. **26**(1), 85–113 (2019)
17. Koch, S., Duvigneau, F., Duczek, S., Woschke, E.: Vibration reduction in automotive applications based on the damping effect of granular material. In: Automotive Acoustics Conference 2017, vol. 102, pp. 43–57. Springer (2019)
18. Kostka, P., Holeczek, K., Hufenbach, W.: Structure-integrated active damping system: integral strain-based design strategy for the optimal placement of functional elements. Int. J. Compos. Mater. **3**(6B), 53–58 (2013)
19. Krause, D., Paetzold, K., Wartzack, S.: Additively manufactured components for structural applications in aircraft interior-two case studies. In: DFX 2016: Proceedings of the 27th Symposium Design for X, pp. 147–156 (2016)
20. Lee, J., Jeon, W.: Vibration damping using a spiral acoustic black hole. J. Acoust. Soc. Am. **141**(3), 1437 (2017)
21. Meyer, N., Schwartz, C., Morlock, M., Seifried, R.: Systematic design of particle dampers for horizontal vibrations with application to a lightweight manipulator. J. Sound Vib. **510** (2021)
22. Sessner, V., Liebig, W.V., Jackstadt, A., et al.: Wide scale characterization and modeling of the vibration and damping behavior of CFRP-elastomer-metal laminates-comparison and discussion of different test setups. Appl. Compos. Mater. **28**(5), 1715–1746 (2021)
23. Storåkers, B.: On material representation and constitutive branching in finite compressible elasticity. J. Mech. Phys. Solids **34**(2), 125–145 (1986)
24. Tan, A.S., Belkner, J., Stroschke, A., Sattel, T.: Damping adjustment utilizing digital electrorheological valves with parallely segmented electrodes. Smart Mater. Struct. **28**(7) (2019)
25. Weaire, D., Fortes, M.A.: Stress and strain in liquid and solid foams. Adv. Phys. **43**(6), 685–738 (1994)

26. Yang, J.S., Ma, L., Schmidt, R., Qi, G., Schröder, K.U., Xiong, J., Wu, L.: Z: hybrid lightweight composite pyramidal truss sandwich panels with high damping and stiffness efficiency. Compos. Struct. **148**, 85–96 (2016)
27. Zhang, D., Qi, T., Zheng, L.: A hierarchical optimization strategy for position and thickness optimization of constrained layer damping/plate to minimize sound radiation power. Adv. Mech. Eng. **10**(10) (2018)
28. Zheng, H., Cai, C., Tan, X.M.: Optimization of partial constrained layer damping treatment for vibrational energy minimization of vibrating beams. Comput. Struct. **82**(29), 2493–2507 (2004)